

Organic field-effect transistors made of epitaxially grown crystals of a thiophene/phenylene co-oligomer**

by Musubu Ichikawa, Hisao Yanagi, Yusuke Shimizu, Shu Hotta, Naotoshi Suganuma, Toshiki Koyama, and Yoshio Taniguchi*

[*] Prof. Y. Taniguchi, Dr. M. Ichikawa, Mr. N. Suganuma, Dr. T. Koyama

Department of Functional Polymer Science

Faculty of Textile Science and Technology

Shinshu University

Tokita 3-15-1, Ueda 386-8567 (Japan)

E-mail: tany@giptc.shinshu-u.ac.jp

Dr. H. Yanagi, Mr. Y. Shimizu

Department of Chemical Science and Engineering

Faculty of Engineering

Kobe University

Rokkodai, Nada-Ku, Kobe 657-8501 (Japan)

Dr. S. Hotta

Institute of Research and Innovation

Kashiwa Laboratory

1201 Takada

Kashiwa, Chiba 277-0861 (Japan)

[**]This work was supported by the New Energy and Industrial Technology Development Organization (NEDO) for Organic Materials Technology for a Solid-State Injection Laser theme. This work was also supported by a Grant-in-Aid for COE Research (10CE2003) from the Japanese Ministry of Education, Culture, Sports, Science, and Technology.

Organic semiconductors are potentially useful materials for optoelectronic devices such as thin-film transistors^[1-4] and light-emitting diodes^[5,6]. We have extensively researched organic semiconductor applications^[7-9] and their device physics,^[10,11] too. Recently, Schön *et al.* have achieved solid-state injection lasing using a tetracene single crystal,^[12] which has demonstrated high practicality of the organic semiconductors. They also demonstrated the potential of organic semiconductors by using single crystalline materials made by vapor phase growth.^[12-15]

Yanagi *et al.* showed that phenylene-oligomers and (thiophene/phenylene)-co-oligomers could be epitaxially grown as a needle-shaped crystal on top of a single crystal substrate of potassium chloride (KCl). The molecular axes of the oligomers were orderly aligned perpendicular to the crystal needle axis.^[16] On the epitaxially grown crystals, self-waveguided light emission takes place along the needle axis^[16,17], and self-waveguided gain-narrowing light emission is also observed^[18]; outstanding optical properties were demonstrated. However, the electric properties of these crystals having such interesting crystal morphology and molecular alignment have been scarcely studied, but it is expected that this molecular alignment is well suited to electric current flow along to the needle axis.

In this paper, we show that the hole mobility of the epitaxially grown crystal of a thiophene/phenylene-co-oligomer is close to that of high-quality molecular single crystals made by vapor phase growth. We also demonstrate that field effect transistors (FETs) made with epitaxially grown crystal have good device characteristics. The thiophene/phenylene-co-oligomer's chemical structure and its notation along with the schematic structure of the fabricated FET are shown in Fig. 1. The FET of Fig. 1(b) was fabricated on top of the SiO₂ layer of the Si wafer used for substrate.

Figure 2 shows an optical microscope image of the resulting FET device. The epitaxially grown BP2T crystals are needle shaped and aligned parallel to each other. Typical dimensions of these crystals are *ca.* 200 nm in thickness, 1 μm in width, and several hundreds of μm in length. As shown in Fig. 2(a), the channel direction of the FET was set to be parallel to the long axis of the needle crystals. Figure 2 also shows a sectional image of the fabricated FET device, where the sectional surface is perpendicular to the needle axis. The wet transferred crystals tightly contact the SiO_2 layer, which acts as a gate insulator. The following should be note here. In addition to the epitaxially grown needle crystals, irregularly shaped matter is visible in the optical image in Fig. 2. Typical dimensions of this matter are $1 \times 5 \mu\text{m}^2$ in area and 100 nm in thickness. Because of their shapes, the matter is probably amorphous and/or small aggregations of microcrystals. In addition, it does not link between the source and drain electrode. Therefore, its electric conduction should be negligible.

Figure 3 shows a set of drain current I_d vs. source-drain voltage V_d curves for various source-gate voltages V_g of the epitaxially grown BP2T FET at room temperature. The device operates in p-channel accumulation and depletion regimes. As shown in the figure, the FET exhibits good operation characteristics, and the characteristics are almost as good as those of single crystalline organic FETs of oligothiophene.^[13] Concretely describing, in each V_g , the leak currents observed at V_d of 0 V are very small, the I_d curves around the V_d of 0 V region are almost ohmic, and the pinch off and saturation characteristics are clearly exhibited.

The field-effect mobility μ_{FET} was estimated from the saturation current, Eq. (1), where L is the channel length, W_{eff} is the "effective" channel width, C_i is the capacitance (per unit area) of the insulator and V_t is the threshold voltage.

$$I_{d,sat} = \frac{W_{eff}}{2L} C_i \mu_{FET} (V_g - V_t)^2, \quad (1)$$

Figure 4 shows the plot of the square root of $I_{d,sat}$ taken at $V_d = -30$ V, as a function of V_g . A mobility of $0.42 \text{ cm}^2\text{V}^{-1}\text{s}^{-1}$ and a threshold voltage of -2.4 V are obtained from linear fitting in Fig. 4. This mobility is considerably small compared with those at room temperature for pentacene evaporated thin films ($1.5 \text{ cm}^2\text{V}^{-1}\text{s}^{-1}$),^[19] polycrystalline thin films ($2.5 \text{ cm}^2\text{V}^{-1}\text{s}^{-1}$),^[20] and single crystals ($3 \text{ cm}^2\text{V}^{-1}\text{s}^{-1}$).^[14] However, the observed mobility is quite larger than that of $2.2 \times 10^{-3} \text{ cm}^2\text{V}^{-1}\text{s}^{-1}$ at room temperature for vacuum deposited thin films of BP2T, and is comparable to that for oligothiophene single crystals,^[13] where all of the mobility is at room temperature. That is, the prepared epitaxially grown organic crystals exhibit good charge transport properties like a single crystal, and therefore, qualities of these crystals are almost close to those of high-quality organic single crystals made by vapor phase growth. Essentially speaking, charge transport characteristics should be discussed on the basis of the temperature dependence of the mobility, and therefore the measurement of the dependence is now in progress.

In addition, this high mobility can be discussed from the viewpoint of the molecular orientation of the epitaxially grown BP2T crystals. Electron diffraction experiments have confirmed that BP2T molecules are orientated perpendicular to the needle axis.^[16] It is well-known that carrier mobility in organic crystals shows anisotropy. For example, carrier mobility in α -sexithiophene single crystals becomes larger for in-plane conduction (a -, b -axis) compared with charge transport perpendicular to the molecular layer (c -axis).^[21] Thus, this high hole mobility may be due to the beneficial molecular orientation.

Figure 4 also shows a semi-logarithmic plot of the drain current at $V_d = -30$ V as a function of V_g . A steep subthreshold slope of 3.1 V/decade and an on/off ratio for

accumulation-depletion operation of 4.4×10^5 could be obtained from the figure, where the on/off ratio was calculated from the drain current ratio at V_g of 10 and -30 V. Geometrical features, the hole mobility, and device operation characteristics of the individual FET devices are summarized in Table 1. We used two different pieces of Si substrate, and this is indicated in the table as Growth 1 and 2. The ratios between the "effective" and "apparent" channel width of individual devices were device-independently about 1:100, because the BP2T crystals for all of the device are prepared at the same epitaxially growth condition. The epitaxial growth in width is an important matter to enhance the device characteristics of our FETs. The hole mobility depended on the device, and the variation of the mobility was from 0.29 to $0.66 \text{ cm}^2\text{V}^{-1}\text{s}^{-1}$. This variation is probably caused by variations not only in geometrical features such as width and thickness of epitaxially grown crystals but also in microscopic differences such as the presence of grain boundaries and the concentrations of defects and impurities. The variations of device operation characteristics are also probably due to these variations. Homogeneity of device characteristics can probably be improved by studying the growth conditions of the crystals.

In conclusion, we have investigated the charge carrier transport property of epitaxially grown thiophene/phenylene-co-oligomer crystal on KCl substrate. As expected from the molecular orientation of the crystal, the crystal shows a good hole transport property. The hole mobility was $0.66 \text{ cm}^2\text{V}^{-1}\text{s}^{-1}$ (maximum), which is relatively close to that of high-quality oligothiophene single crystals made by vapor phase growth. By improving the quality of epitaxially grown crystals, we believe that hole mobility can be made to be as good as that of high-quality molecular single crystals made by vapor phase growth, and also the ambipolar charge transport can be realized.

That epitaxial growth on KCl substrates will be a useful technique for preparation of organic semiconductors.

Experimental

The synthesis and purification methods of BP2T are described in previously published literature.^[22] Crystals of BP2T were epitaxially grown on a KCl (001) substrate by using a hot-wall epitaxy (HWE) method.^[18] These crystals were transferred onto an SiO₂/Si substrate by using a wet transfer method.^[23] For this transfer, the KCl-side surfaces of the grown crystals contacted the SiO₂ surface. The Si substrate (heavily doped p-type, resistibility of 20 – 30 Ωcm) works as a gate electrode, and the thermally grown SiO₂ layer of 400 nm works as a gate dielectric having a capacitance per unit area of 7.5 nF/cm². 50-nm-thick gold electrodes, acting as source and drain electrodes, were thermally evaporated on the BP2T crystals through a shadow mask. The channel length of the FET was 25 μm, and the “apparent” channel width of the FET was set to be 2 or 5 mm. The “apparent” channel width is actually limited by the size of the KCl substrate used for crystal growth. The “effective” channel width (W_{eff}) was estimated from total width of actually connected crystals between the source and drain electrodes under a digital microscope. The FET characteristics of the devices were measured by a source-electrometer (Hewlett-Packard, 4140B). The sectional image of the fabricated FET device was obtained by a focused ion beam apparatus (JEOL, JFIB-2300).

References

- [1] K. Waragai, H. Akimichi, S. Hotta, H. Kano, H. Sakaki, *Phys. Rev. B*, **1995**, 52, 1786.
- [2] G. Horowitz, *Adv. Mater.*, **1998**, 10, 365.
- [3] Z. Bao, *Adv. Mater.*, **2000**, 12, 227.
- [4] C. D. Dimitrakopoulos and P. R. L. Malenfant, *Adv. Mater.*, **2002**, 14, 99.
- [5] V. Bulovic, P. E. Burrows, S. R. Forrest, *Semiconductor and Semimetals*, edited by G. Muller (Academic Press, New York, 1999), Vol. 64, p. ch. 5.
- [6] S. R. Forrest, P. E. Burrows, M. E. Thompson, *IEEE Spectrum*, **2000**, 37, 29.
- [7] A. Yamamori, C. Adachi, T. Koyama, Y. Taniguchi, *J. Appl. Phys.*, **1999**, 86, 4369.
- [8] M. Mitsuya, T. Suzuki, T. Koyama, H. Shirai, Y. Taniguchi, *Appl. Phys. Lett.*, **2000**, 77, 3272.
- [9] M. Ichikawa, Y. Tanaka, N. Suganuma, T. Koyama, Y. Taniguchi, *Jpn. J. Appl. Phys.*, **2001**, 40, L799.
- [10] M. Uchida, C. Adachi, T. Koyama, Y. Taniguchi, *J. Appl. Phys.*, **1999**, 86, 1680.
- [11] M. Ichikawa, R. Naitou, T. Koyama, Y. Taniguchi, *Jpn. J. Appl. Phys.*, **2001**, 40, L1068.
- [12] J. H. Schon, C. Kloc, A. Dodabalapur, B. Batlogg, *Science*, **2000**, 289, 599.
- [13] J. H. Schon, A. Dodabalapur, C. Kloc, B. Batlogg, *Science*, **2000**, 290, 963.
- [14] J. H. Schon, S. Berg, C. Kloc, B. Batlogg, *Science*, **2000**, 287, 1022.
- [15] J. H. Schon, C. Kloc, B. Batlogg, *Nature*, **2000**, 408, 549.
- [16] H. Yanagi, T. Morikawa, S. Hotta, K. Yase, *Adv. Mater.*, **2001**, 13, 313.
- [17] H. Yanagi and T. Morikawa, *Appl. Phys. Lett.*, **1999**, 75, 187.

- [18] H. Yanagi, T. Ohara, T. Morikawa, *Adv. Mater.*, **2001**, *13*, 1452.
- [19] S. F. Nelson, Y.-Y. Lin, D. J. Gundlach, T. N. Jackson, *Appl. Phys. Lett.*, **1998**, *72*, 1854.
- [20] J. H. Schon, C. Kloc, B. Batlogg, *Rhys. Rev. B*, **2001**, *63*, 125304.
- [21] J. H. Schon, C. Kloc, B. Batlogg, *Synth. Met.*, **2000**, *115*, 75.
- [22] S. Hotta, H. Kimura, S. A. Lee, T. Tamaki, *J. Heterocyclic Chem.*, **2000**, *37*, 281.
- [23] Y. Toda and H. Yanagi, *Appl. Phys. Lett.*, **1996**, *69*, 2315.

Figures and Table

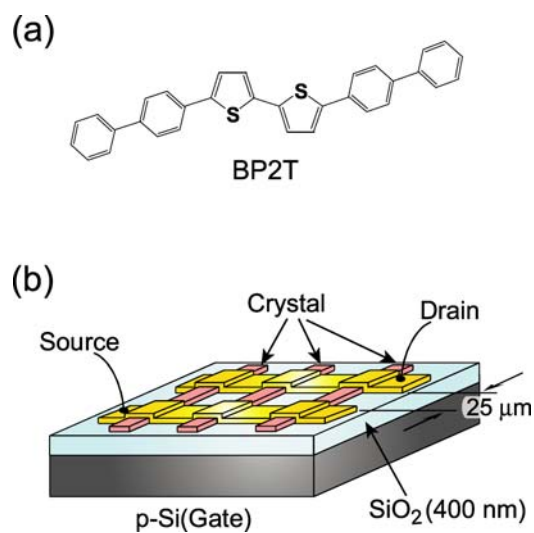


Fig. 1. (a) Structure of and notation for the thiophene/phenylene-co-oligomer used in this study, (b) schematic illustration of the FET device.

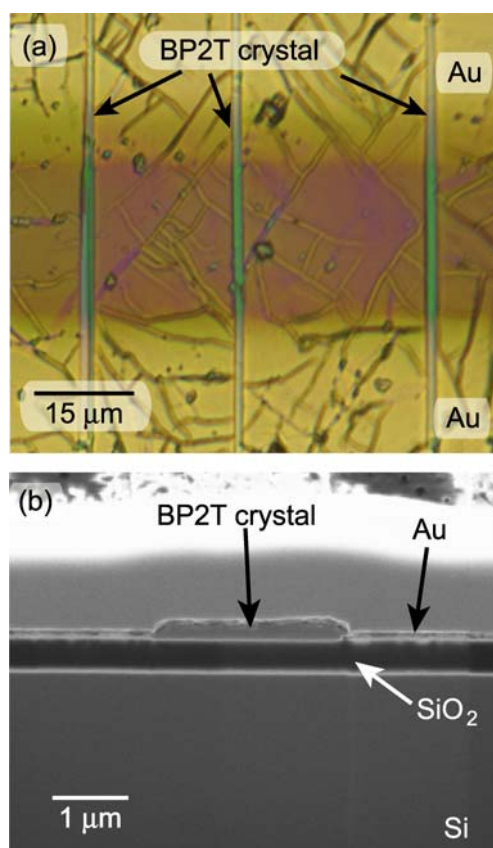


Fig. 2. (a) Optical microscope image of the FET device, (b) sectional image of the FET device.

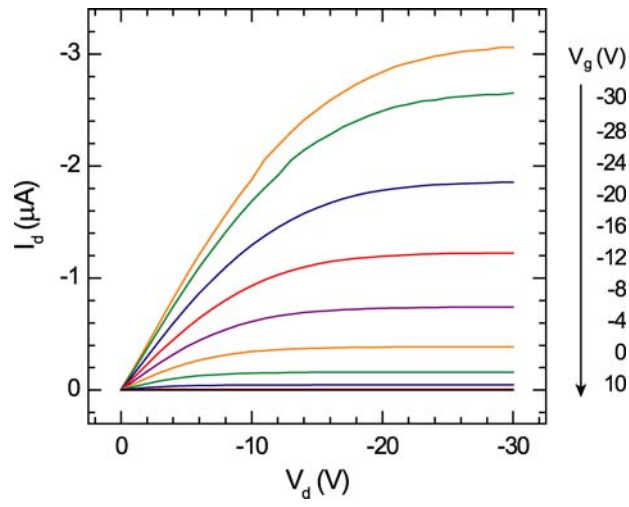


Fig. 3. Drain current I_d vs. source-drain voltage V_d curves for various source-gate voltages V_g of the FET device at room temperature. I_d curves at V_g of 10 and 0 V nearly overlap.

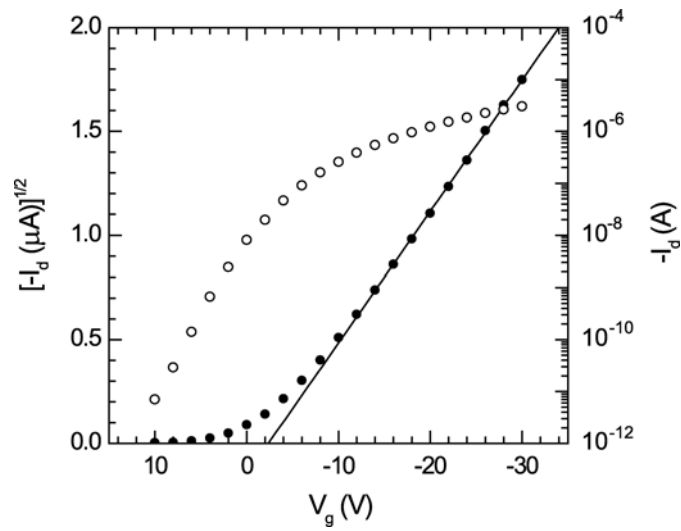


Fig. 4. Transfer characteristics of the FET device at the drain-source voltage V_d of -30 V.

Table 1. Geometrical features, mobility and operation characteristics of individual devices.

| Growth | Device | Apparent channel width (mm) | Effective channel width (μm) | Number of crystals included in the device | Mobility (cm^2/Vs) | Threshold (V) | Steep Subthreshold slope (V/decade) | On/Off ratio ^{a)} |
|--------|--------|-----------------------------|-------------------------------------------|-------------------------------------------|--------------------------------------|---------------|-------------------------------------|----------------------------|
| 1 | 1 | 4.2 | 46.3 | 35 | 0.46 | -5.3 | 3.0 | 9.6×10^3 |
| 1 | 2 | 4.7 | 63.3 | 54 | 0.42 | -2.4 | 3.1 | 4.4×10^5 |
| 1 | 3 | 5 | 38.9 | 35 | 0.66 | -3.9 | 4.4 | 1.9×10^4 |
| 2 | 4 | 2 | 15.1 | 11 | 0.29 | -7.6 | 2.9 | 6.0×10^3 |

^{a)} The on/off ratio, which is calculated from the I_d ratio at V_g of 10 and -30 V, is for accumulation-depletion operation.